

## Timing of rainfall occurrence altered by urban sprawl

Dev Niyogi<sup>a,b</sup>, Krishna K. Osuri<sup>c,\*</sup>, N.K.R. Busireddy<sup>a,c</sup>, Raghu Nadimpalli<sup>d</sup>



<sup>a</sup> Department of Earth Atmosphere and Planetary Sciences, Department of Agronomy, Purdue University, West Lafayette, IN 47907, USA

<sup>b</sup> Jackson School of Geoscience, Department of Geological Sciences and Department of Civil, Architecture, and Environmental Engineering, University of Texas at Austin, Austin, TX, USA

<sup>c</sup> Department of Earth and Atmospheric Sciences, National Institute of Technology Rourkela, Odisha 769 008, India

<sup>d</sup> School of Earth Ocean and Climate Sciences, IIT, Bhubaneswar, Odisha 752 050, India

### ARTICLE INFO

#### Keywords:

Urbanization  
Anthropogenic heat  
WRF model  
Rainfall modification  
Timing of rainfall  
Diurnal rainfall pattern

### ABSTRACT

The impact of urban changes from 1989 to 2015 on urban rainstorms is assessed for the rapidly expanding Indian city of Hyderabad. A typical event that occurred during 12–14 June 2015 is simulated, and the possible association between altered urban-sprawl and shifts in the rainfall timing and patterns are analyzed. The simulation results revealed that the consideration of urban footprint changes was necessary to correctly simulate the heavy rainfall in the high-resolution Weather Research and Forecasting (WRF) model. With the urban expansion and associated anthropogenic heating (AH), the rainfall was more distributed, and its occurrence delayed by ~1–2 h. The results suggest that urbanization can affect rainfall both in terms of the timing as well as the location with respect to the urbanized area. The urban downwind region received an increased rainfall, and this spatial shift was more pronounced with increasing urbanization - from being over the urban area to over rural-urban boundary downwind of the city. The analysis of hydrometeors indicated that rain and cloud quantity decreased with an increasing AH in the urban area. Study results highlight the possibility that the change in the rainfall timing is another climatological signature of urban modification of rainfall.

### 1. Introduction

India is amongst the fastest urbanizing countries in the world. Population growth and increased urbanization associated with land use (LU) land cover (LC) changes (LULCC) are a dominant feature of the surface landscape across India. The changes in the surface characteristics alter the local and regional energetics (Oke, 1982), which interactively modifies regional moisture, albedo, surface roughness, and impact the weather and climate of the region (National Research Council and Climate Research Committee, 2005; Pielke et al., 2011).

In recent years, tropical regions such as India have experienced extreme rainfall events over the megacities (Niyogi et al., 2018). Examples include the iconic July 26, 2005, Mumbai heavy rains (~944 mm of rains within 24 h), and the 2015 Chennai rainfall event (~1049 mm; three times higher than the monthly mean). Studies over the Indian region continue to highlight that unchecked urbanization can lead to unforeseen and increased flood risk (Gupta and Nair, 2010). Studies have also shown that urbanization leads to increased rainfall events and widespread flooding (Kishtawal et al., 2010; Ghosh et al., 2012).

The thermodynamic characteristics of the land surface can alter the surface energy balance and atmospheric boundary layer variations (Niyogi et al., 2006). The anthropogenic changes due to urbanization contribute to the differences in the surface heat

\* Corresponding author.

E-mail addresses: [osurik@nitrkl.ac.in](mailto:osurik@nitrkl.ac.in), [osurikishore@gmail.com](mailto:osurikishore@gmail.com) (K.K. Osuri).

fluxes, boundary-layer heating, and anthropogenic aerosols. A study by Douglas et al. (2009) and several others have reported that the changes in LC characteristics could change the surface albedo, emissivity, and roughness and affect the mesoscale temperature patterns, humidity, convergence and CAPE values (Pielke Sr et al., 2007; Pielke et al., 2011; Osuri et al. 2017). In particular, rapidly growing cities have a high potential to modify the mesoscale features such as local surface climate, circulation patterns, and also the urban hydrological cycle (Collier, 2006; Niyogi, 2019).

The main objective of the study is to assess the role of urbanization on heavy rainfall in terms of timing of initiation, peak activity, spatial distribution, and location of rain intensification using a high-resolution mesoscale model over the rapidly urbanizing city of Hyderabad in southern India. The reason for studying Hyderabad is two-fold. One, it is a rapidly expanding city emblematic of the growth across India, and two, recent observational analysis (Agilan and Umamahesh, 2015) has shown that the sub-daily (4-hourly) extreme rainfall during the non-monsoon months has increased between 1 and 4 a.m. and 5–8 a.m. by 4.5% and 1%, respectively. The observational analysis led to the postulation regarding possible urban and regional climate feedback causing this significant change in the timing of the rainfall around Hyderabad city.

The question we seek to address is whether the evolution in the urban area (urbanization) could have contributed to the changes found in the timing and characteristics of the regional rainfall? The study utilizes detailed modeling experiments using the urbanized version of the WRF (Weather Research and Forecasting, Chen et al., 2011) system to study the possible interplay between urbanization and spatiotemporal rainfall patterns. The numerical experiments are conducted by providing snapshots of landscape characteristics corresponding to Hyderabad urban land cover over different decades as boundary conditions for a representative storm simulation.

## 2. Study region

Hyderabad is the sixth-largest urban agglomerate with a population of 7.5 million (2011 Census of India) located in the southern part of India. The city center is around 17.45°N, 78.46°E, with an elevation of about 500 m from the mean sea level. The city went through rapid urbanization post-1990, with the population increase from 3,906,590 at an annual rate of 2.8% to 5,067,000 in 1999. Through 2000, the population shows a steady growth of 2.7% up to 2014 and eventually crossing the 7 million mark with a census value of 7,609,285. In response to this population growth, the urban extent of Hyderabad has also seen an explosive growth of 7.1% year<sup>-1</sup> between 1990 and 1999 (from 21,668 to 41,958 ha) and 3.7% year<sup>-1</sup> between 1999 and 2014. The urban extent has reached to 72,998 ha by 2014 (<http://www.atlasofurbanexpansion.org/cities/view/Hyderabad>). Fig. 1 shows the urban sprawl footprint over 25 years from the lens of the representative years 1990, 1999, and 2014.

The approach that was taken for selecting the study rainfall cases involved: a review of the storm events from different storm reports, discussions with local experts to ascertain what is a ‘typical’ event that can qualify for doing such a case study, and the availability of observations. Several cases were reviewed initially in the context of what was the primary reason for the heavy rains (large scale event versus mesoscale), availability of measured datasets, and similarity to what is considered typical storms for the regions. After compiling the potential cases, initial WRF runs were conducted for likely candidate storms, and if the model was unable to simulate the broader rainfall features correctly (often due to boundary condition issues), the event was discarded.

Following the preliminary assessment, the analysis discussed ahead builds on a typical rainstorm event from 12 to 14 June 2015. During this period, two different rainfall spells were observed. The first event lasted from 1600 UTC on 12 June to 0000 UTC on 13 June, and the second event started around 1500 UTC on 13 June until 0000 UTC 14 June 2015. The average accumulated rainfall at the end of each period is about 30 mm. This storm event is typical to the city, and also had a good spread of high quality, rain gauge observations from the India Meteorological Department (IMD), and hence considered for additional assessment.

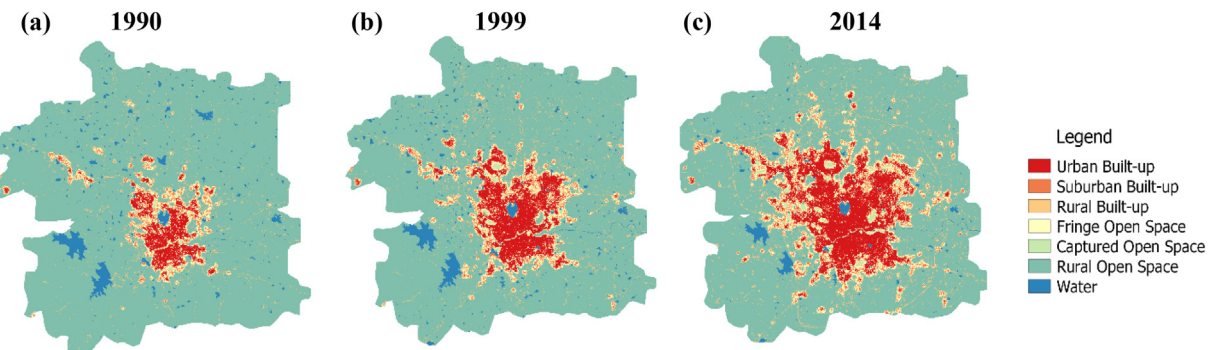


**Fig. 1.** LANDSAT derived urban expansion of Hyderabad corresponding to (a) 1990 (b) 1999 and (c) 2014. Adapted from Angel et al. (2012).

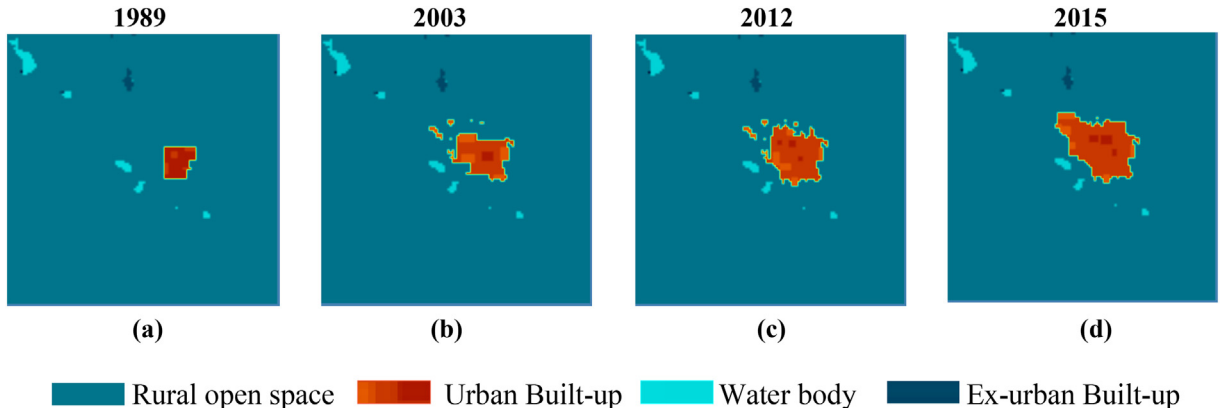


**Fig. 2.** LANSAT derived LULC maps corresponding to (a) 1989 (b) 2003, (c) 2012 and (d) 2015 for use in the WRF simulations.

### 3. Data and methodology

#### 3.1. Data collection and pre-processing

Using Landsat imagery, the LULC maps for 1989, 2003, 2012, and 2015 were developed and are shown in Fig. 2. The default land-type in WRF modeling considers the United States Geological Survey (USGS) 21-category LULC classification system, which was obtained from the Moderate Resolution Imaging Spectroradiometer (MODIS) satellite dataset. For this, the 1 km resolution USGS land cover data extracted from the default WPS geographical data was taken as a reference for the land cover data. After that, ArcGIS10.2.2 was used to generate 1989, 2003, and 2015 land cover maps quantifying the direction and size of the expansion. In this mapping, only the urbanized extent was changed during the processing, and other features such as water bodies and the surrounding croplands were unaltered. The generated urban maps are also in coherence with the LULC maps prepared by Agilan and Umamahesh (2015) and the methodology of Angel et al., (2012). These LULC change maps were further processed using the QGIS software to generate the WPS geog data (as required) for the WRF model simulations. Additional details about viewing, analyzing, and the needed software plug-in (GIS4WRF) to prepare the input data to the WRF model are available in Meyer and Riechert (2019).

Along with these LU maps, the hourly rainfall data of the 28 rain gauges for the rain event period over the Hyderabad city region were obtained from the IMD (Fig. 3).

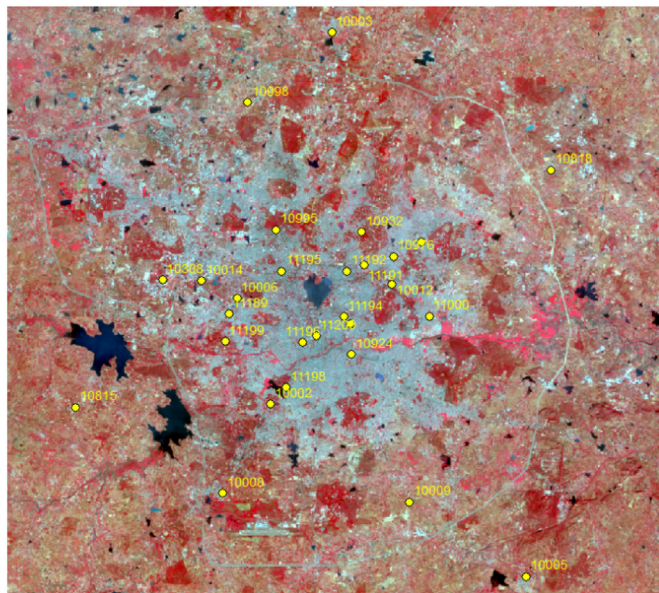


**Fig. 3.** India Meteorological Department rain gauge stations (yellow circles) across Hyderabad city. (For interpretation of the references to colour in this figure legend, the reader is referred to the web version of this article.)

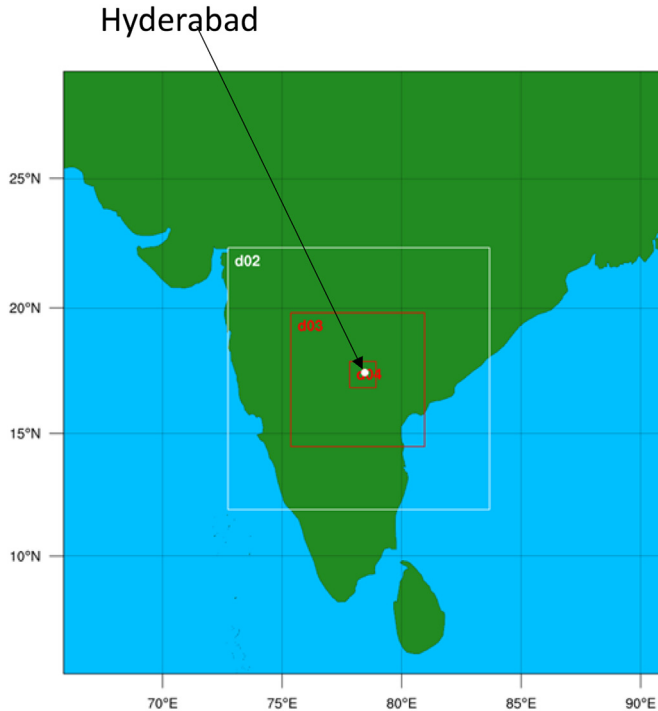


**Fig. 4.** The WRF model configuration with four two-way nested domains. The nested domains d02, d03, and d04 have 9 km, 3 km and 1 km grid spacing. The outermost domain has 27 km grid spacing. The black arrow mark shows the approximate location of Hyderabad city in the d04 domain.

### 3.2. Numerical experiments

The WRF modeling system (Skamarock et al., 2008) is configured with four domains. The horizontal resolution of the parent domain (D01) and nested domains (D02, D03, and D04) are 27 km, 9 km, 3 km, and 1 km, respectively (Fig. 4). Note that the innermost domain (D4) encompasses the Hyderabad city. As a result, the model experiments are conducted focusing on the urban variations within the innermost domains to assess the rainfall modification/changes due to urbanization. The rural grids around the urban areas are also modified accordingly to represent the actual urban extent in the numerical experiments. The numerical model setup and its configuration details are summarized in Table 1 (Janjić, 1994; Chen et al., 2011; Hong et al., 2004; Chen and Dudhia, 2001). Here, the outer domains with relatively coarser grids (D01 and D02) are run with a cloud cumulus parameterization scheme, and for the D03 and D04 domains explicit convection is used. The preliminary experiments provide good results with this configuration setting than that of the domains with the convection physics in all the experiments (see also, Prasad et al., 2014). The initial and boundary conditions for these experiments are obtained from National Centers for Environmental Prediction (NCEP) FNL analysis of  $1^\circ \times 1^\circ$  grid resolution. The static surface data are derived from the United States Geological Survey (USGS) except the land use, which was obtained from the MODIS dataset with 21 land categories at a resolution of 30 arc-second as mentioned earlier.

The four numerical experiments are known as 1989 land use (1989-LU), 2003 land use (2003-LU), 2012 land use (2012-LU), and 2015 land use (2015-LU), respectively. Table 2 provides the percentage of urban sprawl corresponding to the different years (1989, 2003, 2012 and 2015) within the innermost domain. These changes were calculated using the number of pixels corresponding to the urban category divided by the total number of pixels in the innermost (D04) domain. In the default/original geogrid data, there are 13,189 rural grids and 500 urban grids in the reference year, 2012, indicating 3.65% of urban grids in the innermost domain.

**Table 1**

WRF model configuration details.

Spatial horizontal grid spacing (nested domains)	27 km, 9 km, 3 km, and 1 km
Cumulus parameterization	Grell-Devenyi ensemble
PBL scheme	Mellor-Yamada-Janjic (MYJ)
Microphysics	WSM6
Land Surface	Noah LSM with the urban scheme
Surface physics	Monin-Obukhov-Janjic
Long and shortwave radiation	RRTM and Dudhia scheme
Vertical levels	51 in log-linear mode (12 layers within 850 mb and 22 within 500 mb)
Land-use	MODIS-based land cover

**Table 2**

Urban and rural grids in the inner-most (1 km grid spacing, D04) domain for different years. The number in parenthesis indicates the percentage of urban grids in the innermost (D04) domain.

Area/grids	Original Geogrid (Corresponding to the year 2012)	1989	2003	2015
Urban	500 (3.65%)	169 (1.23%)	391 (2.85%)	664 (4.85%)
Rural	13189	13520	13298	13025

Corresponding to this reference year, the percentage of urban sprawl is ~1.23%, 2.85% of urban grids in the years 1989, and 2003. In the year 2015, the urban sprawl has increased to 4.85% for the innermost domain (Table 2). The results show that the urban footprint area steadily increased in 1989, 2003, 2012, and 2015 years, which is consistent with the observations across several cities over India (Lata et al., 2001; Jain et al., 2016). The AH term is considered proportional to the urbanization extent. Therefore, the anthropogenic activities corresponding to the urban sprawl are to be represented realistically to understand the impact of urbanization on rainfall characteristics and is achieved by the ‘anthropogenic heating’ (AH) variable in the WRF model (Kusaka et al., 2012). The WRF model default AH values are  $20 \text{ W m}^{-2}$  (low density),  $50 \text{ W m}^{-2}$  (medium density), and  $90 \text{ W m}^{-2}$  (high density) and corresponds to the year 2012. Corresponding to the changes in urban grids, the default AH has been reduced for the years, 1989 and 2003 LULC cases and increased for 2015 LULC case by the same percentage.

Prior studies have shown that a reliable simulation of urban conditions requires a correct representation of urbanized areas in the weather model (e.g., Ryu et al., 2011). In doing so, there is a notable improvement of the underlying physical processes at and near urban surfaces, primarily through the explicit resolution of urban canopies (e.g., urban canyons and buildings). The thermodynamic properties of the land surface to the atmosphere processes are better explained by the coupling Noah land surface model/Single Layer Urban Canopy Model (LSM/SLUCM). The Noah-LSM is widely used in the coupled atmospheric model as it provides the enthalpy fluxes and surface temperature to the lower boundary conditions. The coupling of the urban canopy model is carried out through the urban percentage ( $Q_{urb}$ ) parameter. It calculates the surface fluxes and temperature from the roofs, walls, trees, and roads. Similarly, the modestly complex SLUCM parameterizes the infinitely long street canyons to show the urban geometry in the form of three-dimensional urban surfaces. The SLUCM accounts for exponential wind profiles, reflections, radiation trapping, shadowing from buildings, heat equations for the road and walls (Chen et al., 2011). It also considers the anthropogenic heating caused due to human activities and its diurnal variations by adding them to the energy balance terms of the urban canopy layer. The calculated sensible heat flux from each urban facet is then passed to the WRF model to show the realistic urban conditions in the lower atmospheric layer (Kusaka et al., 2001; Salamanca et al., 2018).

In addition to these LU change experiments, additional analyses were also undertaken to comprehend the effect of urban physics on using the different land use changes. Table 3 shows the model configuration for three sets of experiments. The first experiment uses the ‘no-urban’ physics; the second one uses urban physics with default AH, and the third considers urban physics with modified AH values. These three experiments hereafter referred to as No-Urb, Urban\_def\_AH, and Urban\_mod\_AH. Note that AH is typically related to urban growth (i.e., larger the city higher the anthropogenic activity and heating). Therefore, Urban\_def\_AH and Urban\_mod\_AH experiments are conducted with the SLUCM model in which it considers the urban footprint more realistically. The Urban\_def\_AH experiment considers the model default AH values and shows LU changes effect over the city. In the case of the Urban\_mod\_AH experiment, the default AH values are modified in such a way that obtained values are proportional to the urbanization footprint change. It calculates the number of cells corresponding to the urban class for each year. Note that 2012-LU is chosen as the reference because it is the default land surface data in the WRF model.

#### 4. Results

An initial analysis is carried out using the No\_Urb and Urban\_def\_AH configurations to understand the rainfall perturbations and its characteristic features. The analysis showed that No\_Urb and Urban\_def\_AH experiments exhibit a similar signature in the rainfall variations. The obtained results are contrary to the available observational evidence (Agilan and Umamahesh, 2015), showing No\_Urb simulation with an increase in rainfall over the city during the day time. Similarly, the Urban\_def\_AH simulation produces rain but it did not exhibit the time delay. It is realized that additional representation of anthropogenic activity and growth in the city is necessary (Lata et al., 2001; Kennedy et al., 2011).

Therefore, additional model runs were carried out to understand the rainfall variations in the model for the increased

**Table 3**

Details of numerical experiments.

Experiment No.	Configuration	LULC	Urban Physics
1. No_urb	cu_physics off in 1 and 3 km domain	LULC change according to LANDSAT imagery	No sfc_urban_physics
2. Urban_def_AH	Same as 1	Same as 1	Considers SLUCM (default AH)
3. Urban_mod_AH	Same as 1	Same as 1	Considers SLUCM with modified AH (proportional to the urbanization extent)

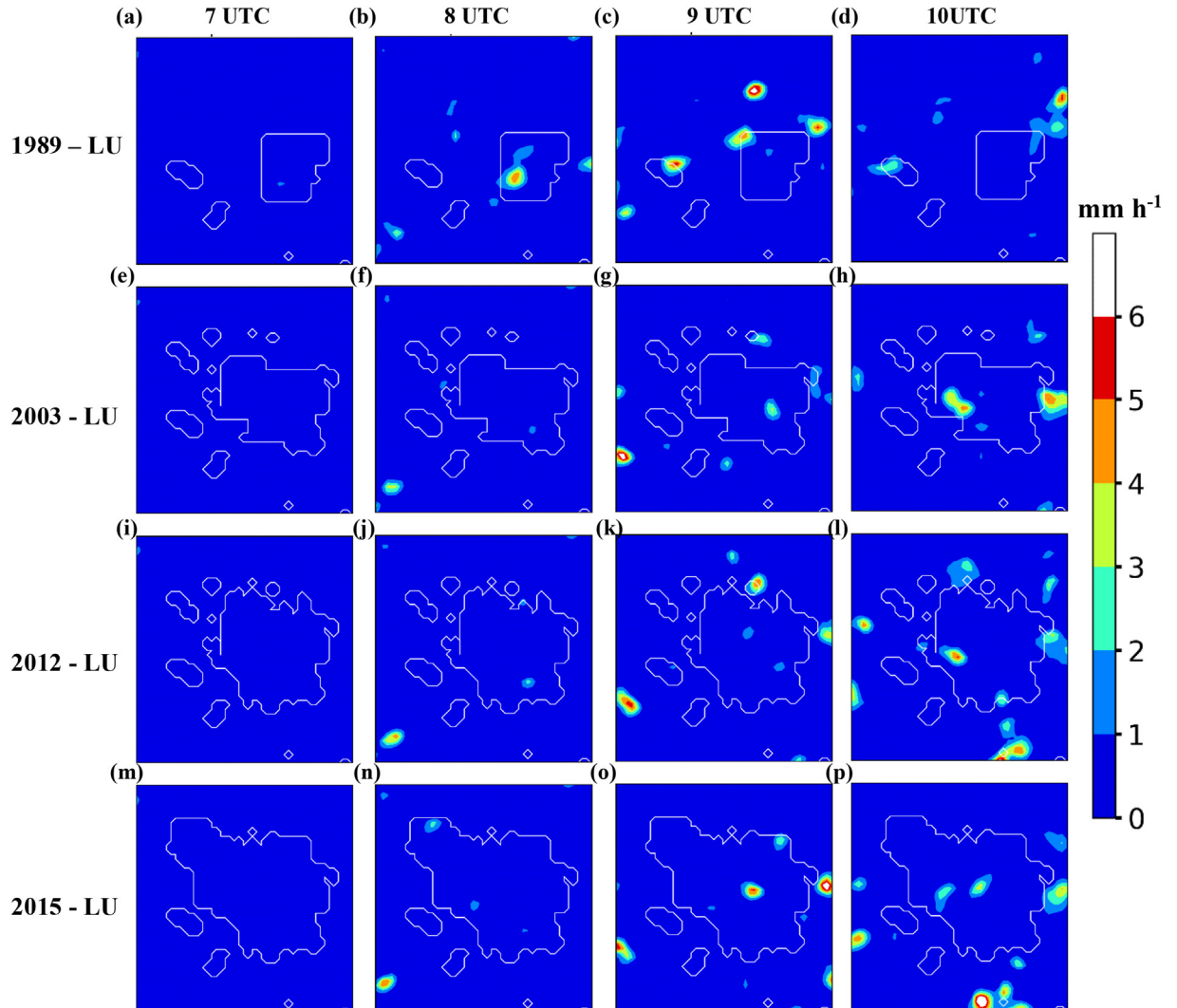


**Fig. 5.** Spatial distribution of hourly rainfall analysis obtained from Urban\_mod\_AH experiments using (a-d) 1989-LU, (e-h) 2003-LU, (i-l) 2012-LU, and (m-p) 2015-LU change values during 7–10 UTC on 11 June 2015. The white contour lines in each sub plot shows the extent of urban area corresponding to that year.

urbanization over the different years. Note that modified or ‘realistic’ AH values are used for this purpose considering a change in the AH relative to the urbanization footprint. Fig. 5 shows the spatial distribution of hourly rainfall using Urban\_mod\_AH values (from 7 to 10 UTC on 11th June 2015). The simulation results show that an increase in the urban footprint delays the rain event over the urban area and its surroundings. For example, the smaller urban footprint of 1989-LU produces a relatively early rainfall as compared to other land use experiments (Fig. 5a-d). The reason behind this early rain is likely due to the reduced AH values (urban footprint) and the corresponding AH quantity is less in the 1989-LU experiment as compared to the 2012-LU. These results suggest that smaller AH could lead to the occurrence of heavy rainfall over the urban area during the rain event period. Correspondingly, the 2003-LU experiment displays a similar amount of rainfall, but the rains occur an hour later (e-h). Likewise, the delay in the heavy rain is also noted in the 2012-LU and 2015-LU experiments (i-p). These results show that rainfall initiated over the urban area decreases in the subsequent hours and further reintensified over the city downwind region after some time (Zhong et al., 2015, 2017). It is also noted in prior observational climatology that the observed amount of rainfall gradually shifts from within a city to its outer periphery (Zhong and Yang, 2015). The overall analysis suggested that the occurrence of a rainfall event is disturbed or delayed by ~2 h due to urbanization.

Fig. 6 shows the hourly rainfall distribution during 16–19 UTC on 13 June 2015. The obtained results appear similar to that for the 11 June 2015 analysis (Fig. 5). Initially, the rain intensity follows the upwind direction and then gradually decreases once it moves towards the urban area (Fig. 6). There is a clear indication of a decrease in rainfall intensity when utilizing the different LU maps starting from 1989-LU to the 2015-LU (Fig. 6a-i). The change is likely due to the pronounced urbanization over the decades that helps to decrease the rainfall activity over the Hyderabad city region. The results highlight that the presence of lower AH and

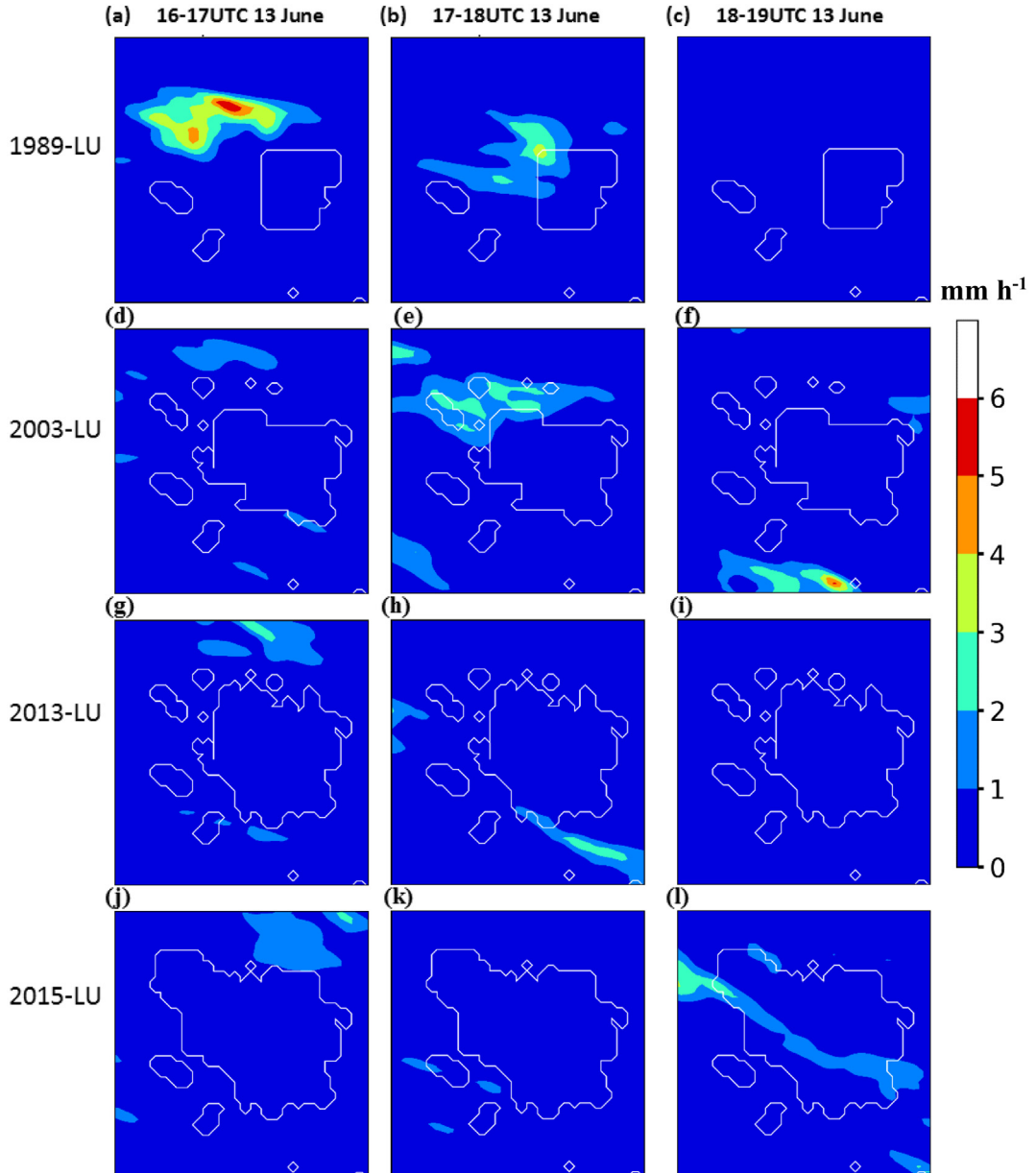


**Fig. 6.** Spatial distribution of hourly rainfall for 16–19 UTC on 13 June 2015 using (a) 1989-LU (b) 2003-LU (c) 2012-LU and (d) 2015-LU changes.

urbanization led to the higher chances of rainfall occurrences over the city, but urban sprawl and anthropogenic heating would likely lead to more rains downwind and lesser rain over the city.

The results are extended further to assess the differences between the default and modified urban anthropogenic heat flux (AH) components in conjunction with the LULC changes. Fig. 7 provides a rainfall comparison between default and modified urban AH during 14–18 UTC 13 June 2015. Note that urban\_mod\_AH uses 2015-LU. The urban\_def\_AH experiment shows intense rainfall pockets in the southeast and northwest region during 15–16 UTC 13 June 2015. The urban\_mod\_AH experiment was unable to produce these features and instead simulated a dry urban locale (Fig. 7b and f). These results further support the recent findings that increase in the urban area led to the rainfall modification over the city which is linked to its anthropogenic heating (Van Den Heever and Cotton, 2007; Hosannah and Gonzalez, 2014). The analysis furthermore revealed persistent rainfall across the city boundaries instead of within the city. These results indicated that higher AH and urbanization could lead to lower rainfall activity over the urban areas, and higher likelihood for rainfall along the downwind urban periphery (Schmid and Niyogi, 2017). The findings align with the perspective discussed in Liu and Niyogi (2019) that with higher urban heat island (UHI) intensity (expected with increased AH), the storms can deflect away from the city causing less rain over the city center and higher rains along the downwind or urban-rural regions. These results again highlight the importance of incorporating realistic AH and urban footprint areas in the models to predict

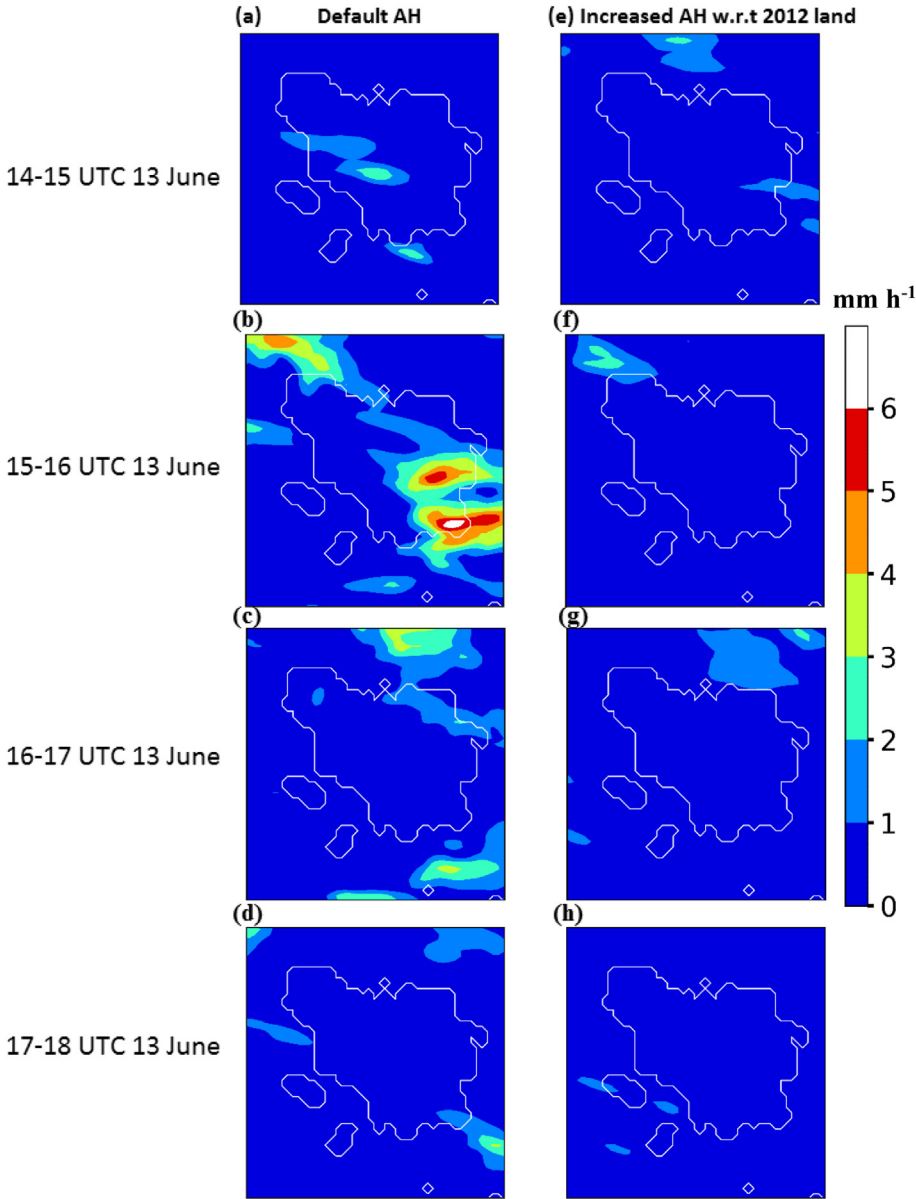


**Fig. 7.** WRF model hourly rain rate simulations with default AH during (a) 14–15 UTC (b) 15–16 UTC (c) 16–17 UTC and (d) 17–18 UTC on 13 June 2015. (e–h) are same as (a–d) but for the modified AH experiment. The solid white contour lines in each figure indicate the city boundaries. Note that these simulations are performed considering the 2015-Land cover as a reference.

or understand the rainfall patterns over the urban regions. [See also a discussion in Yang et al., 2016 on this conclusion but concerning simulating future heatwave impacts over the city].

Fig. 8 shows the time series of averaged rainfall over the urban region corresponding to the various LU (1989, 2003, 2012, and 2015) changes. The No\_Urb physics results simulate rain rate irrespective of the LU changes over the urban region (Fig. 8a). However, the simulated rain rate is not similar for all the three experiments, and a delay in the rain is noticed for increased urbanization. For example, the 1989-LU experiment shows the peak rain rate of  $\sim 2.5 \text{ mm h}^{-1}$  around 17 UTC, whereas the 2003-LU, 2012-LU and 2015-LU changes show the rain rate of  $\sim 3.3$ ,  $\sim 1.7$  and  $\sim 2.3 \text{ mm h}^{-1}$  at 15 and 16 UTC 2013, respectively (Fig. 8a). For the Urban\_def\_AH experiment, the observed peak rainfall episodes for the 1989-LU and 2003-LU were found to be similar to each other, and there was a notable delay by a few hours as compared to the 2015-LU experiment (Fig. 8b). The delay in the rain could be attributed to the higher AH that enhances the UHI with an increased temperature that eventually suppresses the rainfall events (Zhang et al., 2007). A similar experiment is conducted with the help of Urban\_mod\_AH and the results are shown in Fig. 8c. The Urban\_mod\_AH results clearly show the urbanization impact on the rain rate over the city. For instance, the reduced AH values in the 1989-LU experiment results in a heavy rain rate of  $\sim 9.8 \text{ mm h}^{-1}$  as compared to others. The 2003-LU and 2015-LU based rain rate is

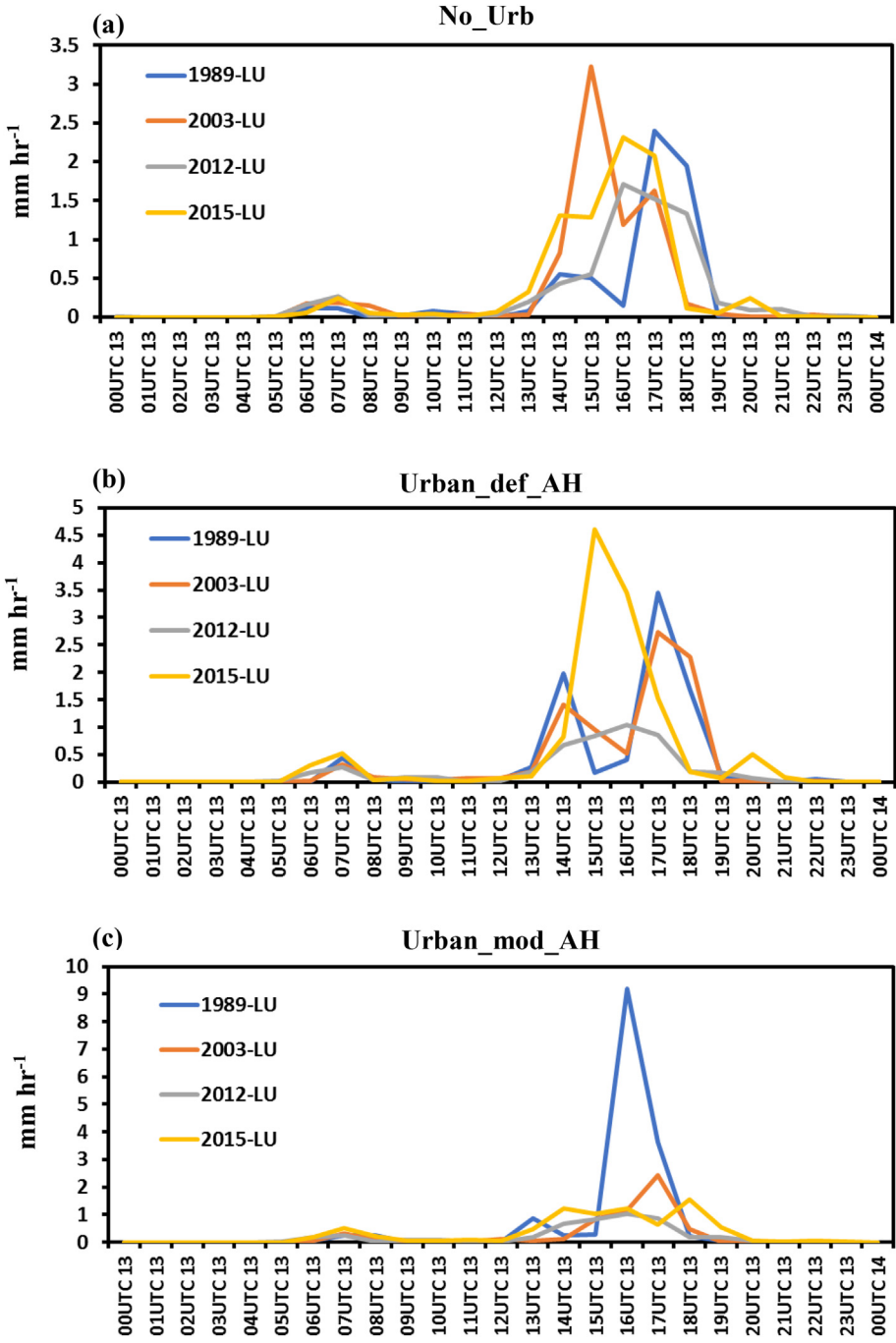


**Fig. 8.** Rainfall time series analysis averaged over the urban area for (a) No urban physics (No\_urb) (b) Urban with default anthropogenic heat (Urban\_def\_AH) and, (c) Urban with modified anthropogenic heat (Urban\_mod\_AH). Note that anthropogenic heat is proportion to an urban extent in the Urban\_mod\_AH experiment.

limited up to 1.8–2 mm h<sup>-1</sup> along with a delay in the rain by 1–2 h in between. The results indicated that urban expansion and modified AH impact the regional urban rainfall both in terms of their spatial location (over the city to downwind) as well as the timing (delay).

To further understand the impact of urban physics on the rainfall variations, vertical cross-sections of the hydrometeors (cloud and rain mixing ratios) during 14–19 UTC on 13 June 2015 using the 2015-LU changes are reviewed. Fig. 9 shows the longitude-height cross-section of the cloud (shaded) and rain (contour) mixing ratios. Note that fields are averaged over a latitudinal band of 17.2°N to 18.0°N to get a better understanding of the thermodynamical processes. The analysis of No\_Urb physics simulation shows

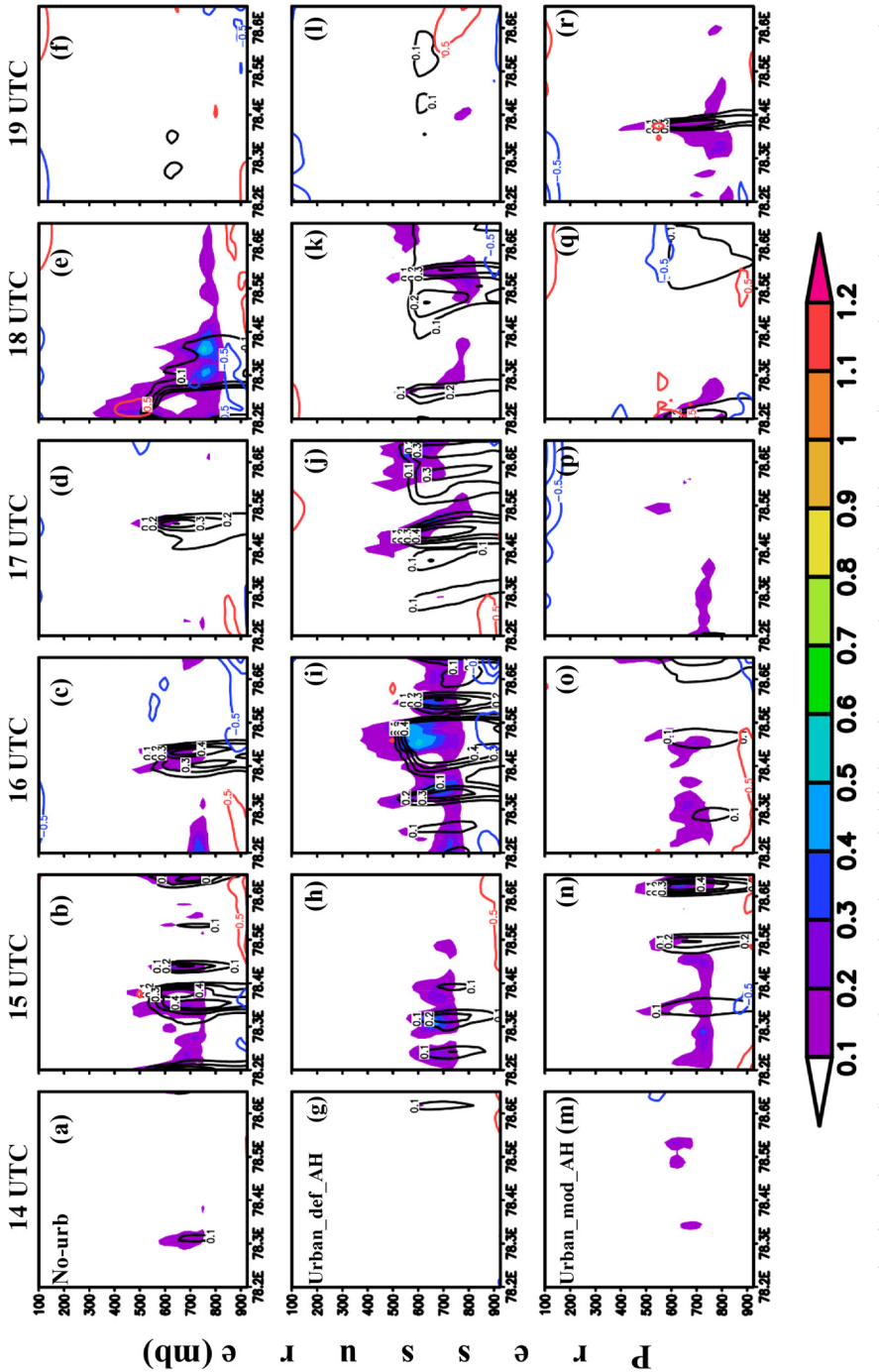


**Fig. 9.** Cloud mixing ratio (g/kg) for (a-f) No urban (No-urb), (g-l) Urban with default anthropogenic heat (Urban\_def\_AH) and, (m-r) Urban with modified anthropogenic heat (Urban\_mod\_AH) experiments. Shaded colour represents the cloud mixing ratio and Red, blue and, black contours corresponds to the heating, cooling and rain mixing ratio (g/kg), respectively. (For interpretation of the references to colour in this figure legend, the reader is referred to the web version of this article.)

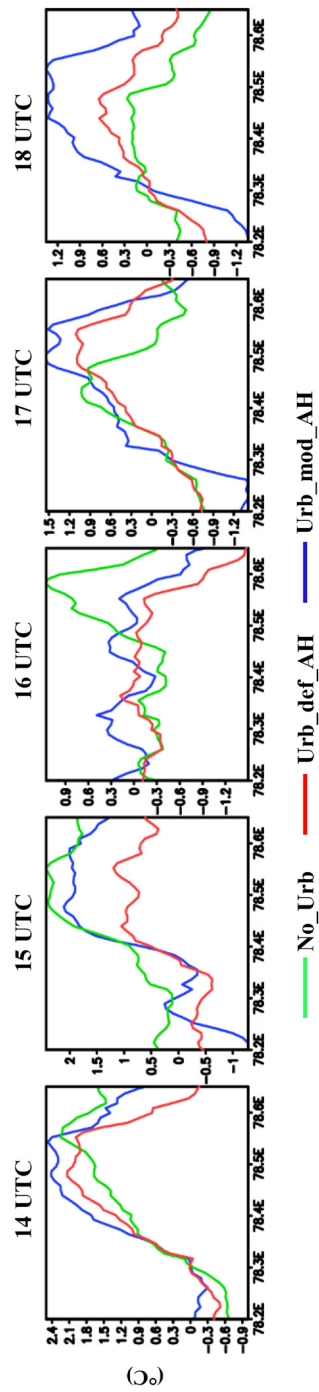


**Fig. 10.** Time series analysis of model simulated temperature anomalies for 13 June 2015 for different hours. The green, red and blue colour lines corresponds to the No\_Urb, Urb\_def\_AH and Urb\_mod\_AH experiments, respectively. (For interpretation of the references to colour in this figure legend, the reader is referred to the web version of this article.)

that the cloud and rain mixing ratios span across rural to urban grids, i.e., 78.2°E to 78.6°E. The maximum horizontal and vertical extent of cloud and rainwater are noted for 18 UTC on 13 June 2015 (Fig. 9a-f). In the case of urban\_def\_AH simulation, the SLUCM (slab) physics produces high values of cloud and rain mixing ratios two hours earlier as compared to the No\_Urb simulation (Fig. 9g-l). Moreover, this rainfall persisted for almost three hours across the region (Fig. 9i-k). A similar analysis with the Urban\_mod\_AH experiment shows that the urban grids suppress the rainfall amounts persistently as compared to other experiments. The decrease in rainfall could be attributed to the ingestion of realistic urban AH values in the model simulations (Agilan and Umamahesh, 2015; Matheson and Ashie, 2008), which leads to changes in the heating rates and causes a divergence potential as discussed in the observational assessment by Dou et al. (2015) considering the urban heating and rainfall deflection from the urban region. Fig. 10 shows the temperature anomalies corresponding to the No\_Urb, Urban\_def\_AH, and Urban\_mod\_AH experiments. These results confirm that surface heating over the urban area is more in the urban\_mod\_AH when compared to the No\_Urb and Urban\_def\_AH experiments (Fig. 10). At the same time, the rural and rural-urban boundaries experience a high rain mixing ratio even though a substantial amount of cloud mixing ratio is present on the urban grids. The overall results highlight the change in the rainfall occurrence with the urban expansion and enhanced urban anthropogenic heating, which inhibits the occurrence of rainfall over the urban area, and shifts it either downwind or cause a delay.

## 5. Conclusions

The study analyzed the effect of urban expansion and its impact on rainfall variations. A representative rainstorm event that occurred during 12–14 June 2015 over the Hyderabad city, India, was considered for detailed numerical experiments using the WRF model.

The consideration of different LULC changes (1989, 2003, 2012, and 2015) in the WRF model revealed that the rainfall occurrence was delayed by ~1–2 h. The analysis showed that the model produced a typically higher rainfall using 1989-LU changes over the urban area. As the urban area and the corresponding AH increased, there was a resulting suppression or delayed rainfall activity over the city. The precipitation over the urban area decreased even though moist convection favored rainfall formation but the convection dissipated shortly likely as a result of the urban heating consistent with the heat island – rainfall discussion presented in Liu and Niyogi (2019) and Dou et al. (2015). An increase in rain intensity was simulated downwind of the city. The analysis of different LULC changes in the model shows a shift in rainfall patterns from over the urban region to the urban-rural boundaries due to urban expansion.

The significance of representing urban physics corresponding to the different LU changes was analyzed using a series of systematic numerical experiments: No-Urb, Urban\_def\_AH, and Urban\_mod\_AH. The results indicated that rainfall received from the Urban\_def\_AH experiment was absent with a change in the AH in the Urban\_mod\_AH. The cloud and rain mixing ratio also showed a decrease in the Urban\_mod\_AH as compared to the Urban\_def\_AH experiment. The presence of high AH leads to heating over the urban region, which through feedbacks, inhibits the rainfall activity before it reaches the ground through the evaporation process (Schmid and Niyogi, 2013). The analysis provides a consistent signature of urban influence on the clouds and rainfall patterns over the city region.

These findings are likely to be of interest to the broader urban climate community for hydroclimatology and flooding issues. In this study, Hyderabad city is taken as an example, but many other urbanized locales in India (e.g., Rupa and Mujumdar, 2018), as well as other parts of the world (e.g., Yu and Liu, 2015), are expected to display this signature of change in rainfall timing post urbanization. Given the lack of dense rainfall datasets, these results provide a tantalizing opportunity to detect the climatological impact of urbanization on rainfall not just by changes in the spatial structure but also by reviewing change of the rainfall timing from a sparse rain gauge network.

## Author statement

The authors of the manuscript entitled “Timing of Rainfall Occurrence Altered by Urban Sprawl” hereby declare that they do not have any conflicts of interest for this publication in your premium journal. We declare that the work undertaken in the mentioned research article has not been submitted elsewhere earlier and is not under review by any other journal.

## Declaration of Competing Interest

The authors of the manuscript entitled “Timing of Rainfall Occurrence Altered by Urban Sprawl” hereby declare that they do not have any conflicts of interest for this publication in your premium journal.

## Acknowledgments

The study benefitted through financial support from the U.S. NSF grants: OAC-1835739, AGS-1522494, and AGS-1902642, and USDA Hatch Project at Purdue University. We also acknowledge the financial support from Earth System Science Organization, Ministry of Earth Sciences (MoES/16/14/2014-RDEAS), Govt. of India; and SERB (ECR/2016/001637) Govt. of India. The third author also acknowledges the SERB-Purdue OVDF program (SB/S9/Z-03/2017) for support of the visit to Purdue University. The discussions with Dr. V. Agilan, National Institute of Technology Warangal during the course of this study is also acknowledged.

## References

- Agilan, V., Umamahesh, N.V., 2015. Detection and attribution of non-stationarity in intensity and frequency of daily and 4-h extreme rainfall of Hyderabad, India. *J. Hydrol.* 530, 677–697.
- Angel, S., Blei, A.M., Civco, D.L., Parent, J., 2012. *Atlas of Urban Expansion*. Lincoln Institute of Land Policy, Cambridge, MA, pp. 397.
- Chen, F., Dudhia, J., 2001. Coupling an advanced land surface-hydrology model with the Penn State-NCAR MM5 modeling system. Part I: model implementation and sensitivity. *Mon. Weather Rev.* 129 (4), 569–585.
- Chen, F., Kusaka, H., Bornstein, R., Ching, J., Grimmond, C.S.B., Grossman-Clarke, S., Loridan, T., Manning, K.W., Martilli, A., Miao, S., Sailor, D., 2011. The integrated WRF/urban modelling system: development, evaluation, and applications to urban environmental problems. *Int. J. Climatol.* 31 (2), 273–288.
- Collier, C.G., 2006. The impact of urban areas on weather. *Q. J. R. Meteorol. Soc.* 132 (614), 1–25. Available at: <https://doi.org/10.1256/qj.05.199>.
- Dou, J., Wang, Y., Bornstein, R., Miao, S., 2015. Observed spatial characteristics of Beijing urban climate impacts on summer thunderstorms. *J. Appl. Meteorol. Climatol.* 54 (1), 94–105.
- Douglas, E.M., Beltrán-Przekurat, A., Niyogi, D., Pielke Sr., R.A., Vörösmarty, C.J., 2009. The impact of agricultural intensification and irrigation on land-atmosphere interactions and Indian monsoon precipitation—a mesoscale modeling perspective. *Glob. Planet. Chang.* 67 (1–2), 117–128.
- Ghosh, S., Das, D., Kao, S.C., Ganguly, A.R., 2012. Lack of uniform trends but increasing spatial variability in observed Indian rainfall extremes. *Nat. Clim. Chang.* 2 (2), 86.
- Gupta, A.K., Nair, S.S., 2010. Flood risk and context of land-uses: Chennai city case. *J. Geogr. Region Plan.* 3 (12), 365–372.
- Hong, S.Y., Dudhia, J., Chen, S.H., 2004. A revised approach to ice microphysical processes for the bulk parameterization of clouds and precipitation. *Mon. Weather Rev.* 132 (1), 103–120.
- Hosannah, N., Gonzalez, J.E., 2014. Impacts of aerosol particle size distribution and land cover land use on precipitation in a coastal urban environment using a cloud-resolving mesoscale model. *Adv. Meteorol.* 2014.
- Jain, M., Dimri, A.P., Niyogi, D., 2016. Urban sprawl patterns and processes in Delhi from 1977 to 2014 based on remote sensing and spatial metrics approaches. *Earth Interact.* 20 (14), 1–29.
- Janjić, Z.I., 1994. The step-mountain eta coordinate model: further developments of the convection, viscous sublayer, and turbulence closure schemes. *Mon. Weather Rev.* 122 (5), 927–945.
- Kennedy, L., Robbins, G., Scott, D., Sutherland, C., Denis, E., Andrade, J., Bon, B., 2011. The politics of large-scale economic and infrastructure projects in fast-growing cities of the south. *Lit. Rev. 3 Online document available at: [http://chance2sustain.eu/fileadmin/Website/Dokumente/Dokumente/Publications/C2S\\_WP2\\_litRev\\_The\\_Politics\\_of\\_Large-Scale\\_Economic.pdf](http://chance2sustain.eu/fileadmin/Website/Dokumente/Dokumente/Publications/C2S_WP2_litRev_The_Politics_of_Large-Scale_Economic.pdf)*
- Kishtawal, C.M., Niyogi, D., Tewari, M., Pielke Sr., R.A., Shepherd, J.M., 2010. Urbanization signature in the observed heavy rainfall climatology over India. *Int. J. Climatol.* 30 (13), 1908–1916.
- Kusaka, H., Kondo, H., Kikegawa, Y., Kimura, F., 2001. A simple single-layer urban canopy model for atmospheric models: comparison with multi-layer and slab models. *Bound.-Layer Meteorol.* 101 (3), 329–358.
- Kusaka, H., Chen, F., Tewari, M., Dudhia, J., Gill, D.O., Duda, M.G., Wang, W., Miya, Y., 2012. Numerical simulation of urban heat island effect by the WRF model with 4-km grid increment: an inter-comparison study between the urban canopy model and slab model. *J. Meteorol. Soc. Japan. Ser. II* 90, 33–45.
- Lata, K.M., Rao, C.S., Prasad, V.K., Badarianth, K.V.S., Raghavasamy, V., 2001. Measuring urban sprawl: a case study of Hyderabad. *GIS Develop.* 5 (12), 26–29.
- Liu, J., Niyogi, D., 2019. Meta-analysis of urbanization impact on rainfall modification. *Sci. Rep.* 9 (1), 7301. <https://www.nature.com/articles/s41598-019-42494-2>.
- Matheson, M.A., Ashie, Y., 2008. The effect of changes of urban surfaces on rainfall phenomenon as determined by a non-hydrostatic mesoscale model. *J. Meteorol. Soc. Japan. Ser. II* 86 (5), 733–751.
- Meyer, D., Riechert, M., 2019. Open source QGIS toolkit for the advanced research WRF modelling system. *Environ. Model. Softw.* 112, 166–178.
- National Research Council, Climate Research Committee, 2005. *Radiative Forcing of Climate Change: Expanding the Concept and Addressing Uncertainties*. National Academies Press.
- Niyogi, D., 2019. Land surface processes. In: *Current Trends in the Representation of Physical Processes in Weather and Climate Models*. Springer, Singapore, pp. 349–370.
- Niyogi, D., Holt, T., Zhong, S., Pyle, P.C., Basara, J., 2006. Urban and land surface effects on the 30 July 2003 mesoscale convective system event observed in the southern Great Plains. *J. Geophys. Res. Atmos.* 111 (D19).
- Niyogi, D., Subramanian, S., Mohanty, U.C., Kishtawal, C.M., Ghosh, S., Nair, U.S., Ek, M., Rajeevan, M., 2018. The impact of land cover and land use change on the Indian monsoon region hydroclimate. In: *Land-Atmospheric Research Applications in South and Southeast Asia*. Springer, Cham, pp. 553–575.
- Oke, T.R., 1982. The energetic basis of the urban heat island. *Q. J. R. Meteorol. Soc.* 108 (455), 1–24.
- Osuri K., K., Nadimpalli, R., Mohanty, U.C., Chen, F., Rajeevan, M., Niyogi, D., 2017. Improved prediction of severe thunderstorms over the Indian Monsoon region using high-resolution soil moisture and temperature initialization. *Sci. Rep.* 7, 41377. <https://doi.org/10.1038/srep41377>.
- Pielke Sr., R.A., Adegoke, J., Beltrán-Przekurat, A., Hiemstra, C.A., Lin, J., Nair, U.S., Niyogi, D., Nobis, T.E., 2007. An overview of regional land-use and land-cover impacts on rainfall. *Tellus Ser. B Chem. Phys. Meteorol.* 59 (3), 587–601.
- Pielke, R.A., Pitman, A., Niyogi, D., Mahmood, R., McAlpine, C., Hossain, F., Goldeijk, K.K., Nair, U., Betts, R., Fall, S., Reichstein, M., 2011. Land use/land cover changes and climate: modeling analysis and observational evidence. *Wiley Interdiscip. Rev. Clim. Chang.* 2 (6), 828–850.
- Prasad, S.K., Mohanty, U.C., Routray, A., Osuri, K.K., Ramakrishna, S.S.V.S., Niyogi, D., 2014. Impact of Doppler weather radar data on thunderstorm simulation during STORM pilot phase—2009. *Nat. Hazards* 74 (3), 1403–1427.
- Rupa, C., Mujumdar, P.P., 2018. Dependence structure of urban precipitation extremes. *Adv. Water Resour.* 121, 206–218.
- Ryu, Y.H., Baik, J.J., Lee, S.H., 2011. A new single-layer urban canopy model for use in mesoscale atmospheric models. *J. Appl. Meteorol. Climatol.* 50 (9), 1773–1794.
- Salamanca, F., Zhang, Y., Barlage, M., Chen, F., Mahalov, A., Miao, S., 2018. Evaluation of the WRF-urban modeling system coupled to Noah and Noah-MP land surface models over a semiarid urban environment. *J. Geophys. Res. Atmos.* 123 (5), 2387–2408.
- Schmid, P.E., Niyogi, D., 2013. Impact of city size on precipitation-modifying potential. *Geophys. Res. Lett.* 40 (19), 5263–5267.
- Schmid, P.E., Niyogi, D., 2017. Modeling urban precipitation modification by spatially heterogeneous aerosols. *J. Appl. Meteorol. Climatol.* 56 (8), 2141–2153.
- Skamarock, W.C., Klemp, J.B., Dudhia, J., Gill, D.O., Barker, D.M., Wang, W., Powers, J.G., 2008. A Description of the Advanced Research WRF Version 3. NCAR Technical note-475+ STR.
- Van Den Heever, S.C., Cotton, W.R., 2007. Urban aerosol impacts on downwind convective storms. *J. Appl. Meteorol. Climatol.* 46 (6), 828–850.
- Yang, J., Wang, Z.H., Georgescu, M., Chen, F., Tewari, M., 2016. Assessing the impact of enhanced hydrological processes on urban hydrometeorology with application to two cities in contrasting climates. *J. Hydrometeorol.* 17 (4), 1031–1047.
- Yu, M., Liu, Y., 2015. The possible impact of urbanization on a heavy rainfall event in Beijing. *J. Geophys. Res. Atmos.* 120 (16), 8132–8143.
- Zhang, C.L., Chen, F., Miao, S.G., Li, Q.C., Xuan, C.Y., 2007. Influences of urbanization on precipitation and water resources in the metropolitan Beijing area. In: *Proceedings of the 21st American Meteorological Society Conference on Hydrology*. vol. 17 San Antonio, TX, USA.
- Zhong, S., Yang, X., 2015. Ensemble simulations of the urban effect on a summer rainfall event in the great Beijing metropolitan area. *Atmos. Res.* 153, 318–334.
- Zhong, S., Qian, Y., Zhao, C., Leung, R., Yang, X.Q., 2015. A case study of urbanization impact on summer precipitation in the greater Beijing metropolitan area: urban heat island versus aerosol effects. *J. Geophys. Res. Atmos.* 120 (20).
- Zhong, S., Qian, Y., Zhao, C., Leung, R., Wang, H., Yang, B., Fan, J., Yan, H., Yang, X.Q., Liu, D., 2017. Urbanization-induced urban heat island and aerosol effects on climate extremes in the Yangtze River Delta region of China. *Atmos. Chem. Phys.* 17 (8), 5439–5457.